Polarization dynamics in VCSELs subject to optical frequency comb injection

Yaya Doumbia, Delphine Wolfersberger, Krassimir Panajotov, Marc Sciamanna

Polarization dynamics in VCSELs subject to optical frequency comb injection

Yaya Doumbia[a,b], Delphine Wolfersberger[a,b], Krassimir Panajotov[c,d], and Marc Sciamanna[a,b]

[a]Chaire Photonique, LMOPS, CentraleSupélec, Metz, France
[b]Université de Lorraine, CentraleSupélec, LMOPS, Metz, France
[c]Brussels Photonics Group (B-PHOT), Vrije Universiteit Brussel, Brussels, Belgium
[d]Institute of Solid State Physics, Bulgarian Academy of Sciences, Sofia, Bulgaria

ABSTRACT

In this work, we experimentally and theoretically report on optical comb dynamics in VCSELs induced by optical injection. We show that injection of a narrow comb with parallel, orthogonal or arbitrary polarization can sustain two polarization comb dynamics in single-mode VCSELs. More specifically, we show that the two polarization comb dynamics can be observed whatever the injected comb's polarization. The appearance of the comb can be controlled with the linewidth enhancement factor for fixed injected comb spacing and detuning frequency. Also, we show that the harmonics comb in the two orthogonal polarization modes can be suppressed with the linewidth enhancement factor in the cases of parallel and orthogonal optical injection.

Keywords: Optical frequency comb, Polarization dynamics, Nonlinear dynamics, Optical injection, VCSELs

1. INTRODUCTION

Optical frequency comb technologies have attracted much attention due to their numerous applications ranging from integrated photonics, optical metrology, optical communication, frequency comb spectroscopy, and frequency comb LIDAR. Optical frequency comb originate from the so called mode-locked laser.[1] Since their discovery, the optical combs have focused intense scientific research theoretically and experimentally.[2,3] These activities have led to several physical system generating optical frequency comb such as electro-optics modulator, microresonator and semiconductor lasers. The semiconductors lasers employed for optical comb generation include the quantum cascade laser,[2–4] quantum dot lasers,[5,6] and Vertical-Cavity Surface-Emitting Lasers (VCSELs).[7,8] Most importantly, the rich nonlinear dynamics in semiconductor lasers[9–15] make them perfect candidates for optical comb generation.[16]

In particular, VCSEL based-optical frequency comb has driven much attention recently due to its compactness, low energy consumption, possibility of integration, and mass production. Besides these advantages, VCSELs provide interesting nonlinear dynamics and polarization properties[17–24] linked to the cylindrical geometry of their cavity combined with the symmetry of the gain in the plane of quantum wells. The properties of the gain medium of the VCSELs give rise to a week polarization anisotropy that leads to emission and selection of two preferential orthogonal polarization directions. Most VCSELs are single longitudinal mode, i.e., they emit light along only one of the two orthogonal polarization directions. The polarization mode that contains the maximum power (minimum power) is called the dominant polarization mode (depressed polarization mode). In addition, depending on the operation conditions, polarization modes instabilities such as polarization switching and polarization bistability may be observed in the VCSEL output. The polarization switching and the related bistability have been first observed in free-running VCSEL when varying the injection current and the temperature.

More recently, polarization switching has been demonstrated in VCSEL under orthogonal optical injection.[25–30] The optical injection consists to transmitted a portion of light from a laser called *master* laser into the cavity of a second laser called *slave* laser. Interestingly, it has been shown that polarization switching

Further author information: (Send correspondence to A.A.A.)
A.A.A.: E-mail: aaa@tbk2.edu, Telephone: 1 505 123 1234
B.B.A.: E-mail: bba@cmp.com, Telephone: +33 (0)1 98 76 54 32

can bifurcate to nonlinear wave-mixing, complex dynamics, period one dynamics, period-doubling dynamics, high-order periodic dynamics, and chaotic dynamics.[31–33,33,34] In addition, VCSELs have even shown complex polarization dynamics in free-running.[23] Single-mode optical injection in semiconductor lasers has driven a lot of attention during several decades. Recent studies have paid a lot of attention to the optical injection dynamics in semiconductor lasers from optical frequency combs.[35,36] More specifically, optical comb injection has unveiled several nonlinear dynamics in diode lasers such as optical injection locking with selective amplification, harmonics frequency locking, relaxation oscillation frequency locking,[37] and extension of the injected comb to a much broader optical spectrum.[38,39] Some recent works have taken advantage of the polarization properties in VCSEL to control the injection locking and the injected comb properties.[40,41]

It is also shown that parallel or orthogonal optical injection in single-mode VCSEL can enable two polarization comb dynamics. The comparison between the polarization comb dynamics induced by parallel and orthogonal optical in VCSEL is lacking.

This paper provides an in-depth analysis of nonlinear polarization dynamics in VCSEL subject to optical comb injection. More specifically, we experimentally and theoretically analyze the polarization dynamics in VCSEL under parallel and orthogonal optical injection when varying the SFM parameters. We show that the impact of the SFM parameters on the two polarization comb dynamics depends on the polarization of injected comb lines.

2. EXPERIMENTAL RESULTS

Figure 1 (a) shows the experimental setup used to analyze the polarization dynamics in a VCSEL under orthogonal, parallel, and arbitrary optical injection. The output of a tunable laser (TL) is amplified by an Erbium-Doped Fiber Amplifier (EDFA) and then sent to the RF port of the Mach-Zehnder Modulator (MZM). The polarization controller at the input of the MZM allows aligning its polarization with the tunable laser output. The MZM is driven with an Arbitrary Waveform Generator (AWG). Three optical frequency lines are generated at the output of the MZM. A fiber circulator provides isolation for optical injection in VCSEL. The total power of the injected comb is controlled with a Variable Optical Attenuator (VOA). The optical spectra are analyzed with a BOSA, and the corresponding time series are displayed with an Electrical spectrum analyzer (ESA). The two polarization controllers combined with the polarized beam splitter allows analyzing the polarization-resolved optical spectra of the VCSEL. Our previous publications provide more details on the acquisition systems.[40,41]

Figure 1 (b), shows the optical spectrum of the injected comb for injected comb spacing of $\Omega = 2$ GHz. The difference, in dB, between the power of the central frequency line and the others frequency lines is around 12 dB. Figure 1 (c), shows the optical spectrum of the VCSEL in free-running. Figure 1 (c) is obtained for injection current of 6 mA. Our previous publications[40,41] provide more details on the characteristic of the VCSEL. The frequency detuning $\Delta\nu$ is measured from the frequency position of the central injected comb line to the frequency of dominant polarization mode (X-PM) of the VCSEL, i.e., $\Delta\nu = \nu_0 - \nu_x$, where ν_0 and ν_x are the frequencies of the central injected comb line and the X-polarization mode (X-PM) of VCSEL, respectively.

The polarization dynamics in a single-mode VCSEL are analyzed in Fig. 2. Figure 2 is measured for injected comb spacing of $\Omega = 2$ GHz. As we have learned from our previous manuscript,[40–43] injection of a narrow optical frequency comb with parallel or orthogonal polarization can sustain a two polarization comb dynamics in a single-mode VCSEL. For fixed injection parameters, i.e., detuning frequency of $\Delta\nu = -17$ GHz and injected power of $P_{inj} = 248.8$ µW, we analyzed the impact of the polarization of the injected comb on the two polarization comb dynamics. Figure 2 shows that the two polarization comb dynamics are not restricted to the cases of parallel or orthogonal optical injection. Interestingly, when varying the polarization of the injected comb from the orthogonal optical injection to parallel optical injection, we observe that the total number of comb line decreases. For these injection parameters, the best comb properties are found when the polarization of the injected comb is orthogonal to that of the VCSEL.

3. NUMERICAL SIMULATIONS

The optical injection in VCSEL is modeled using the so-called SFM, which takes into account the light polarization properties.[34] We consider an injection configuration in which the two polarization modes of the VCSEL are

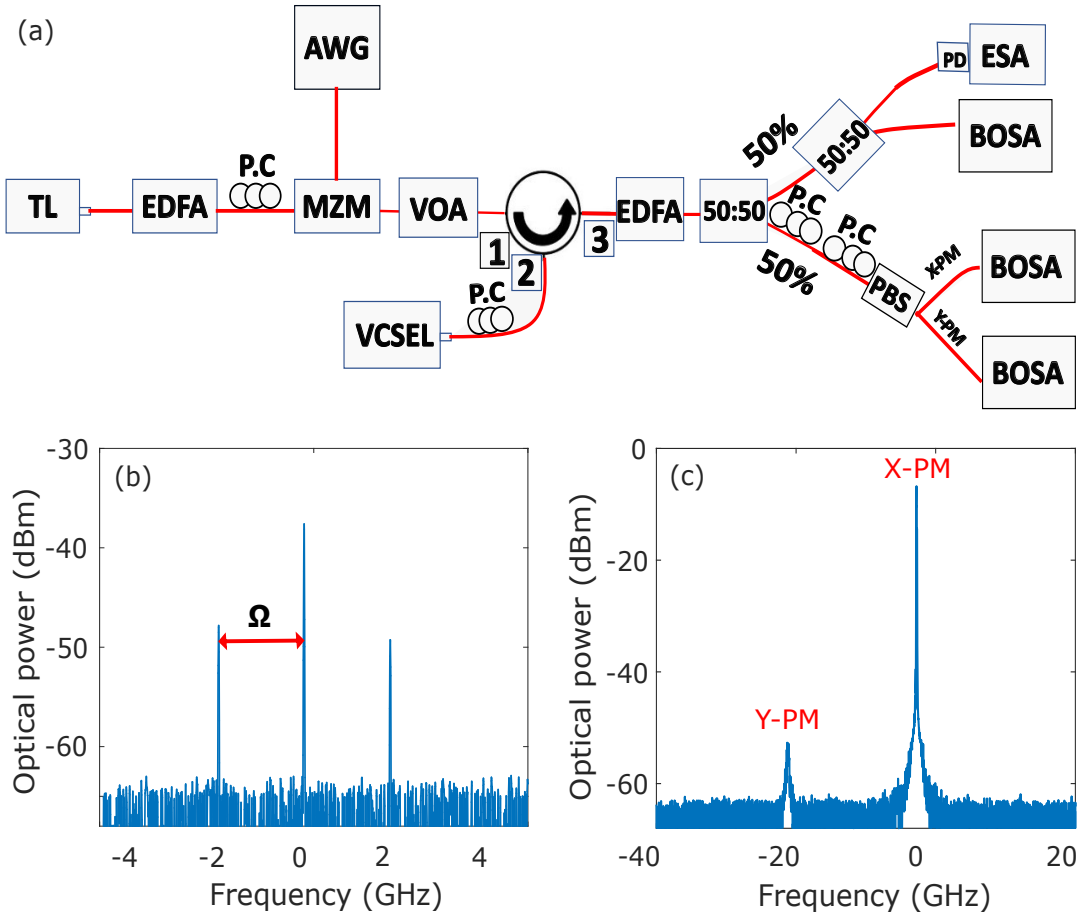

Figure 1. Setup for optical comb injection. TL: Tunable Laser, EDFA: amplifier, P.C: Polarization Controller, AWG: Arbitrary Waveform Generator, MZM: Mach-Zehnder Modulator, VOA: Variable Optical Attenuator, OSA: Optical Spectrum Analyser, PD: photodiode, ESA: Electrical spectrum analyzer. (b), and (c) correspond to the optical spectra of the injected comb and VCSEL in free-running, respectively. The injected comb spacing is $\Omega = 2$ GHz.

affected by the injected field. The SFM parameters are chosen such that the free-running VCSEL emits along with the X-polarization mode (X-PM). Parallel (orthogonal) optical injection corresponds to the situation where the polarization of the injected field is parallel (Orthogonal) to that of the VCSEL. The rate equation of the VCSEL under optical injection can be written as:

$$\frac{dE_x}{dt} = -(\kappa + \gamma_a)E_x - i(\kappa\alpha + \gamma_p)E_x + \kappa(1 + i\alpha)(DE_x + inE_y) + Injx * E_M, \tag{1}$$

$$\frac{dE_y}{dt} = -(\kappa - \gamma_a)E_y - i(\kappa\alpha - \gamma_p)E_y + \kappa(1 + i\alpha)(DE_y - inE_x) + Injy * E_M, \tag{2}$$

$$\frac{dD}{dt} = -\gamma[D(1 + |E_x|^2 + |E_y|^2) - \mu + in(E_yE_x^* - E_xE_y^*)], \tag{3}$$

$$\frac{dn}{dt} = -\gamma_s n - \gamma[n(|E_x|^2 + |E_y|^2) + iD(E_yE_x^* - E_xE_y^*)]. \tag{4}$$

In these equations, E_x and E_y correspond to the components of the complex electrical field of the polarization modes X and Y, respectively. D and n correspond to the two carriers variable. μ is the normalized injection current. γ_p, γ_a, and γ_s are the linear birefringence, linear dichroism, and the spin-flip relaxation rate, respectively,

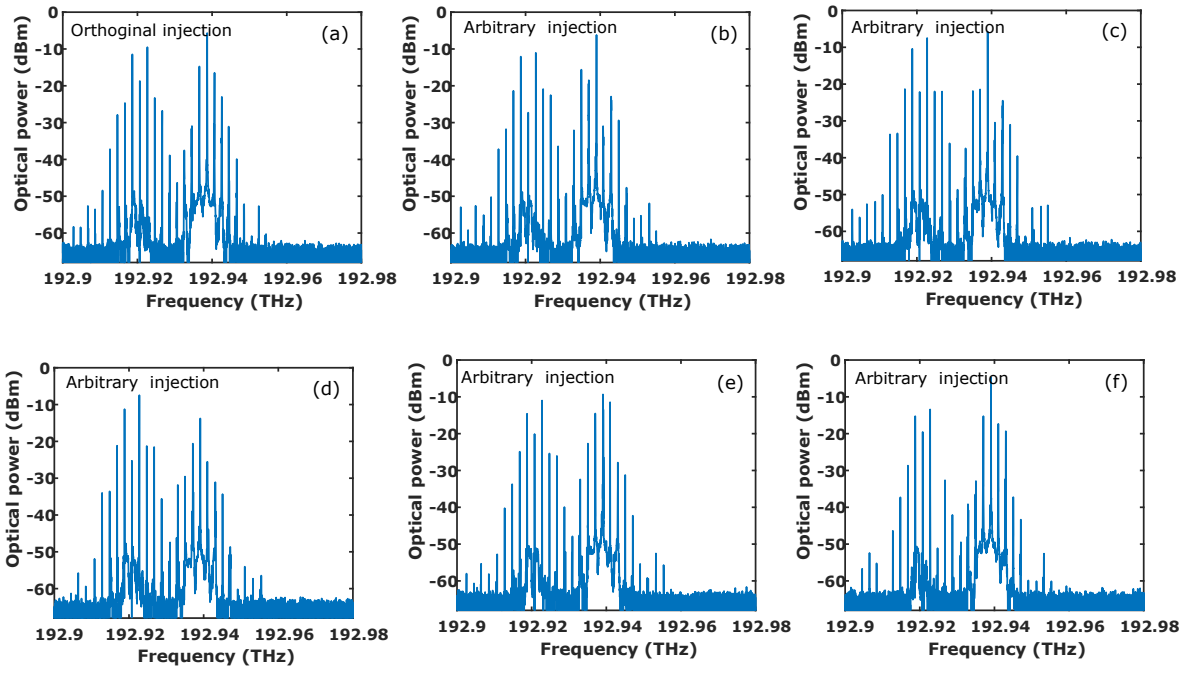

Figure 2. Nonlinear polarization dynamics in a single-mode VCSEL with optical frequency comb injection. The injected comb spacing is $\Omega = 2$ GHz. These optical spectra are obtained for fixed detuning $\Delta\nu = -17$ GHz and injected power of $P_{inj} = 248.8$ µW. (a) correspond to the orthogonal optical injection while (b)-(f) are obtained for an arbitrary polarized comb injection.

γ is the decay rate of D, κ is the field decay rate, and α is the linewidth enhancement factor (alpha parameters). The following equation gives the electrical field of the injected comb:

$$E_M = \kappa_{inj} \sum_j E_j(t) e^{i(2\pi\nu_j t + \varphi_j(t))} \tag{5}$$

where ν_j is the frequency and E_j the amplitude of the j_{th} injected comb lines, κ_{inj} the coupling coefficient. We suppose that $\kappa_{inj} = \kappa$, which corresponds to an optimal coupling between the VCSEL output and the injected comb lines. We also suppose that the phase of individual injected comb lines is zero, i.e., $\varphi_j = 0$. The detuning frequency $\Delta\nu_j$ is the difference between the injected comb lines, ν_j and the intermediate frequency between those of the X and Y polarization, $\frac{2\pi\nu_x + 2\pi\nu_y}{2}$, with $2\pi\nu_x = \alpha\gamma_a - \gamma_p$ and $2\pi\nu_y = \gamma_p - \alpha\gamma_a$, the frequency corresponding to the linear polarization mode X and Y, respectively. Inj_x and Inj_y allow to ensure parallel or orthogonal optical injection. To achieve parallel optical injection we set $Inj_x = 1$ and $Inj_y = 0$ while orthogonal optical corresponds to the situation where $Inj_x = 0$ and $Inj_y = 1$.

The SFM parameters used in the simulations are summarized in table 1 : These numerical value are taken

κ	33 ns^{-1}	The field decay rate
γ_a	-0.1 ns^{-1}	The linear dichroism
α	2.8	Linewidth enhancement factor
μ	2.29	The normalized bias current
γ_p	9 GHz	The linear birefringence
γ	2.08 ns^{-1}	The decay rate of D
γ_s	2100 ns^{-1}	The spin-flip relaxation rate

Table 1. The semiconductor laser parameters and their numerical value.

from.[32] In the following, we shall use κ_{inj} as injection strength, with $\kappa_{inj} = \frac{E_{inj}}{E_0}$. E_{inj} and E_0 are the total amplitude of the injected comb and the total amplitude of the free-running VCSEL. The SFM model (1-4) is numerically integrated using a fourth-order Runge-Kutta method. The numerical simulations are performed for a long time series of 200 ns with a times step of 1.2 ps. The detuning frequency referred to as $\Delta\nu$ will always be defined from the central injected comb line. The injected comb is a narrow optical comb with three frequencies line. To realistically model our experimental configuration in,[40–43] we consider that the difference between the amplitudes of the injected comb lines is 12 dB. Figure 3 shows the polarization-resolved optical spectra of X-polarization mode (X-PM) and Y-polarization mode (Y-PM), respectively. We inject the 3-comb lines in either the dominant or the normally depressed polarization mode.

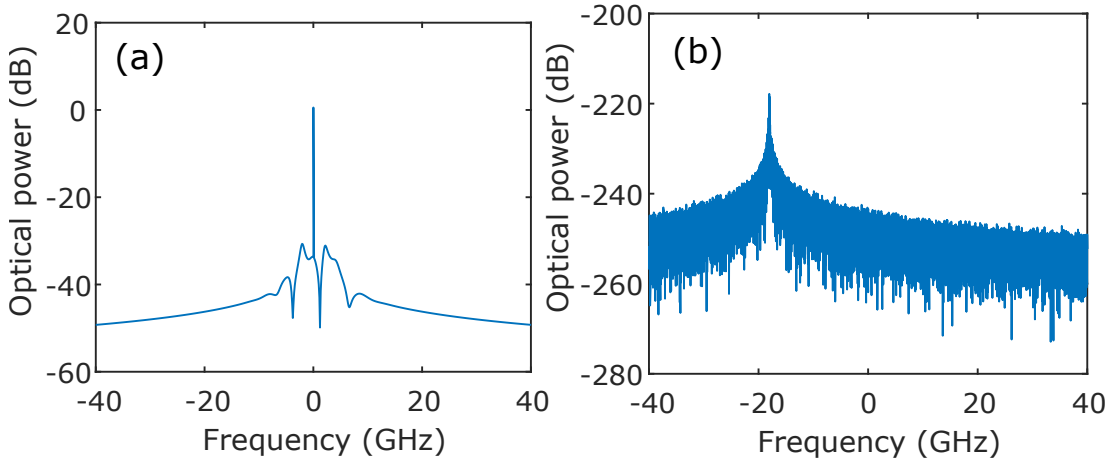

Figure 3. Polarization resolved optical spectra of free-running VCSEL. (a) and (b) show the optical spectra of X-polarization mode (X-PM) and Y-polarization mode (Y-PM), respectively.

3.1 Parallel optical injection

Our previous experimental and theoretical investigations have demonstrated the possibility of generating two polarization combs from a single-mode VCSEL. More specifically, when the polarization of the injected comb is turned to be orthogonal or parallel to that of the VCSEL, the polarization switching or excitation of the depressed polarization mode can be accompanied by two combs generation with orthogonal polarization directions.

Figure 4 analyzes the two polarization comb dynamics in VCSEL under parallel optical injection when varying the linewidth enhancement factor. The injected comb spacing is fixed to $\Omega = 2$ GHz and detuning frequency $\Delta\nu_x = -9$ GHz. The bifurcation diagrams in Figure 4 are obtained by selecting the maxima and minima of polarization-resolved intensities $I_{x,y} = |E_{x,y}|^2$ for each injection strength. In Figure 4, the blue and red correspond to the bifurcation diagrams of X-PM and Y-PM, respectively. Figure 4 (a) plots the bifurcation diagram for $\alpha = 1$. At low injection strength, a nonlinear wave-mixing occurs only in X-polarization mode. Like in,[38–41] this wave-mixing appears at the detuning frequency and a new frequency that depends on the injected comb spacing. When the injection strength reaches $\kappa = 0.4$, the depressed polarization mode (Y-PM) is abruptly excited, accompanied by optical comb generation. Interestingly, the dominant polarization mode (X-PM) remains stable with the generation of another optical comb. These two polarization combs have the same repetition rate as the injected one. The two combs with orthogonal polarization remain stable over a wide range of injection strength and then bifurcate to the harmonics frequency lines simultaneously. These harmonics comb lines allow controlling the two polarization comb repetition rate. Figure 4 (a) shows the bifurcation of the polarization-resolved intensities when $\alpha = 2$. We observe that the region of nonlinear wave-mixing at low injection strength has decreased, but one of the two polarization combs remains almost the same. Unlike Fig. 4 (a) where the two polarization comb bifurcates to harmonics comb generation. The black arrows indicate the harmonics comb regions. Fig. 4 (b) shows that the increase in α destabilize the VCSEL to the complex dynamics generation in the dominant polarization mode. When we keep increasing α, the size of the two polarization comb

dynamics decreases to give rise to the complex dynamics only in the dominant polarization mode (X-PM) as shown in Fig. 4 (c) and (d).

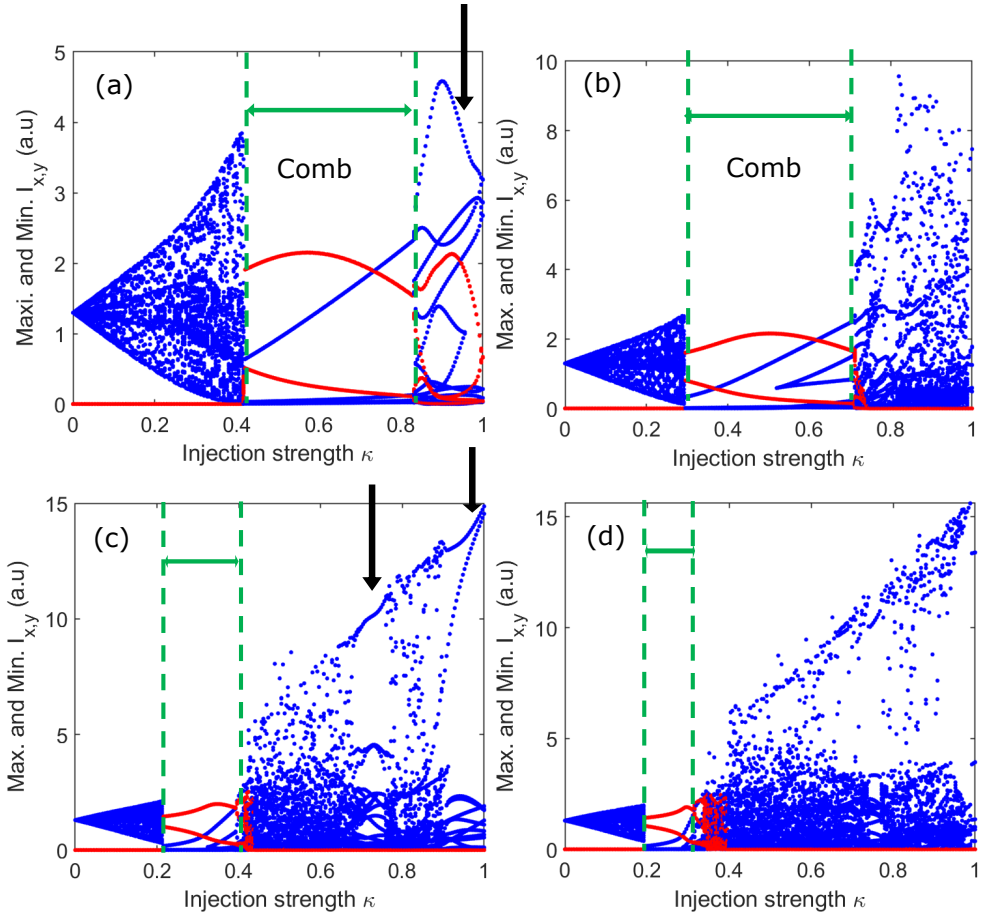

Figure 4. Bifurcation diagrams of VCSEL under parallel optical frequency comb. These bifurcation diagrams are obtained for fixed injected comb spacing of $\Omega = 2$ GHz and detuning frequency of $\Delta\nu_x = -9$ GHz. The blue and red colors correspond to the bifurcation of X-polarization mode (X-PM) and Y-polarization mode (Y-PM), respectively. (a), (b), (c), and (d) are obtained for $\alpha = 1$, $\alpha = 2$, $\alpha = 4$ and $\alpha = 5$, respectively. The two polarization comb regions are indicated between the two vertical dashed lines.

3.2 Orthogonal optical injection

We next turned the polarization of the injected comb to be orthogonal to that of the VCSEL. Figure 5 analyzes the bifurcation diagram for orthogonal optical injection in VCSEL when varying the linewidth enhancement factor. These bifurcation diagrams are obtained for the same detuning frequency and injected comb spacing as Fig. 4. Unlike the case of parallel optical injection where a nonlinear wave-mixing in X-PM leads to the two polarization comb dynamics, Fig. 5 shows the polarization switching with two combs generation with the orthogonal polarization direction. The two vertical dashed lines indicate the two polarization comb regions in the bifurcation diagrams. Like Fig. 4, the size of the comb regions decreases with the increase in the linewidth enhancement factor. The two polarization comb disappears at $\alpha = 5$ [see Fig. 5 (d)]. When we keep increasing the linewidth enhancement factor, harmonics comb dynamics take place in the depressed polarization mode as shown in Fig. 5 (c) and (d). The black vertical arrows indicate the harmonic comb regions in the bifurcation diagrams.

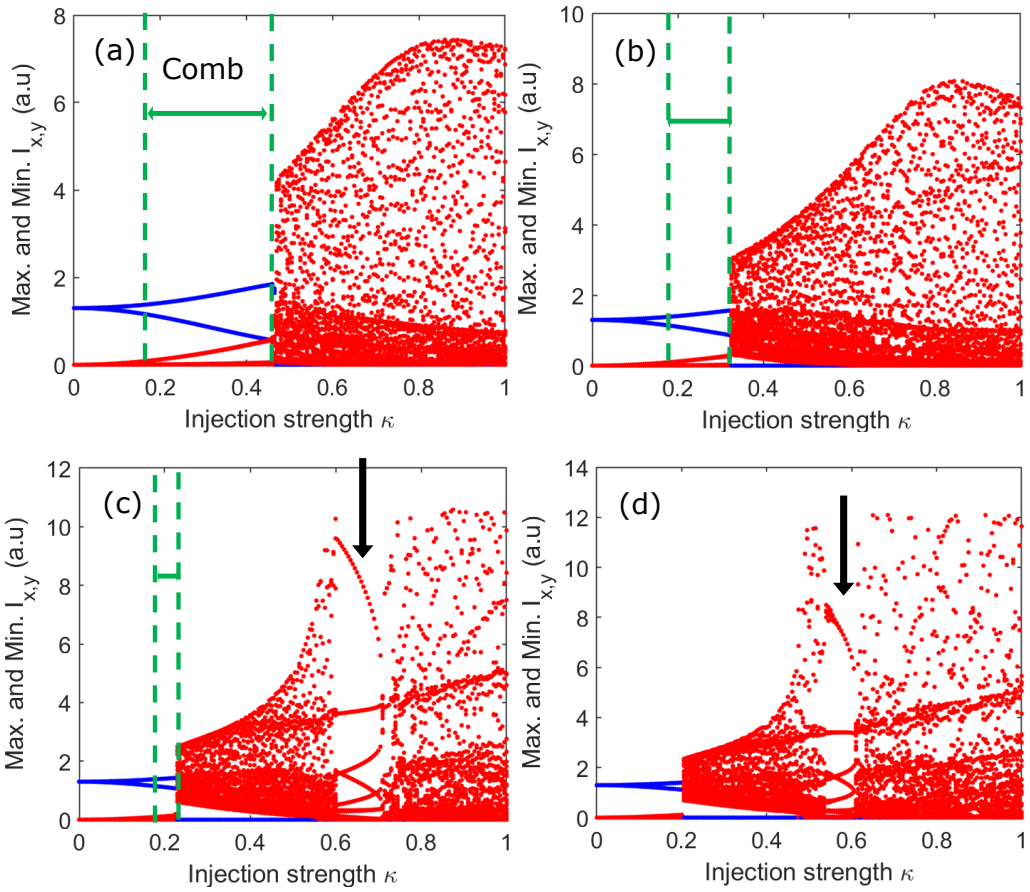

Figure 5. Bifurcation diagrams for orthogonal optical injection in a single-mode VCSEL. These bifurcation diagrams are obtained for fixed injected comb spacing of $\Omega = 2$ GHz and detuning frequency of $\Delta\nu_x = -9$ GHz. The blue and red colors correspond to the bifurcation of X-polarization mode (X-PM) and Y-polarization mode (Y-PM), respectively. (a), (b), (c), and (d) are obtained for $\alpha = 1$, $\alpha = 2$, $\alpha = 4$ and $\alpha = 5$, respectively. The two polarization comb regions are indicated between the two vertical dashed lines. The vertical black arrows indicate the harmonics comb dynamics regions.

4. CONCLUSION

We have shown experimentally and theoretically that optical comb injection can sustain two combs with orthogonal polarization direction in single-mode VCSELs. We have also demonstrated that the two polarization comb dynamics are observed, whatever the injected comb's polarization. For detuning frequency of $\Delta\nu = -17$ GHz, the best two polarization comb is found when the polarization of the injected comb is orthogonal to that of the VCSEL. We have numerically highlighted the impact of the linewidth enhancement factor on the two polarization comb dynamics. We have also shown that the size of the two polarization comb dynamics region is controllable with the linewidth enhancement factor.

Funding : The presented study is funded by the Chaire Photonique: Ministère de l'Enseignement Supérieur, de la Recherche et de l'Innovation; Région Grand-Est; Département Moselle; European Regional Development Fund (ERDF); GDI Simulation; CentraleSupélec; Fondation CentraleSupélec. Fondation Supélec and Metz Metropole. Fonds Wetenschappelijk Onderzoek (FWO) Vlaanderen Project No.G0E5819N.

REFERENCES

[1] Hargrove, L., Fork, R. L., and Pollack, M., "Locking of he–ne laser modes induced by synchronous intracavity modulation," *Applied Physics Letters* **5**(1), 4–5 (1964).

[2] Hugi, A., Villares, G., Blaser, S., Liu, H., and Faist, J., "Mid-infrared frequency comb based on a quantum cascade laser," *Nature* **492**(7428), 229–233 (2012).

[3] Silvestri, C., Columbo, L. L., Brambilla, M., and Gioannini, M., "Coherent multi-mode dynamics in a quantum cascade laser: amplitude-and frequency-modulated optical frequency combs," *Optics Express* **28**(16), 23846–23861 (2020).

[4] Villares, G., Hugi, A., Blaser, S., and Faist, J., "Dual-comb spectroscopy based on quantum-cascade-laser frequency combs," *Nature communications* **5**(1), 1–9 (2014).

[5] Weber, C., Columbo, L. L., Gioannini, M., Breuer, S., and Bardella, P., "Threshold behavior of optical frequency comb self-generation in an inas/ingaas quantum dot laser," *Optics letters* **44**(14), 3478–3481 (2019).

[6] Grillot, F., Duan, J., Dong, B., and Huang, H., "Uncovering recent progress in nanostructured light-emitters for information and communication technologies," *Light: Science & Applications* **10**(1), 1–17 (2021).

[7] Quirce, A., de Dios, C., Valle, A., and Acedo, P., "Vcsel-based optical frequency combs expansion induced by polarized optical injection," *IEEE Journal of Selected Topics in Quantum Electronics* **25**(6), 1–9 (2018).

[8] Ren, H., Fan, L., Liu, N., Wu, Z., and Xia, G., "Generation of broadband optical frequency comb based on a gain-switching 1550 nm vertical-cavity surface-emitting laser under optical injection," in [*Photonics*], **7**(4), 95, Multidisciplinary Digital Publishing Institute (2020).

[9] Mogensen, F., Olesen, H., and Jacobsen, G., "Locking conditions and stability properties for a semiconductor laser with external light injection," *IEEE Journal of Quantum Electronics* **21**(7), 784–793 (1985).

[10] Sciamanna, M. and Shore, K. A., "Physics and applications of laser diode chaos," *Nature photonics* **9**(3), 151–162 (2015).

[11] Erneux, T., [*Applied delay differential equations*], vol. 3, Springer Science & Business Media (2009).

[12] Kovanis, V., Gavrielides, A., Simpson, T., and Liu, J.-M., "Instabilities and chaos in optically injected semiconductor lasers," *Applied physics letters* **67**(19), 2780–2782 (1995).

[13] Jumpertz, L., Schires, K., Carras, M., Sciamanna, M., and Grillot, F., "Chaotic light at mid-infrared wavelength," *Light: Science & Applications* **5**(6), e16088–e16088 (2016).

[14] Olejniczak, L., Panajotov, K., Thienpont, H., and Sciamanna, M., "Self-pulsations and excitability in optically injected quantum-dot lasers: Impact of the excited states and spontaneous emission noise," *Physical Review A* **82**(2), 023807 (2010).

[15] Tabaka, A., Panajotov, K., Veretennicoff, I., and Sciamanna, M., "Bifurcation study of regular pulse packages in laser diodes subject to optical feedback," *Physical Review E* **70**(3), 036211 (2004).

[16] Larsson, A., "Advances in vcsels for communication and sensing," *IEEE Journal of selected topics in quantum electronics* **17**(6), 1552–1567 (2011).

[17] Sciamanna, M., Panajotov, K., Thienpont, H., Veretennicoff, I., Mégret, P., and Blondel, M., "Optical feedback induces polarization mode hopping in vertical-cavity surface-emitting lasers," *Optics letters* **28**(17), 1543–1545 (2003).

[18] Panajotov, K., Sciamanna, M., Arteaga, M. A., and Thienpont, H., "Optical feedback in vertical-cavity surface-emitting lasers," *IEEE Journal of Selected Topics in Quantum Electronics* **19**(4), 1700312–1700312 (2012).

[19] Panajotov, K., Sciamanna, M., Gatare, I., Arizaleta Arteaga, M., and Thienpont, H., "Nonlinear dynamics of vertical-cavity surface-emitting lasers," *Advances in Optical Technologies, Volume 2011, Article ID 469627* (2011).

[20] Altés, J. B., Gatare, I., Panajotov, K., Thienpont, H., and Sciamanna, M., "Mapping of the dynamics induced by orthogonal optical injection in vertical-cavity surface-emitting lasers," *IEEE journal of quantum electronics* **42**(2), 198–207 (2006).

[21] Hurtado, A., Quirce, A., Valle, A., Pesquera, L., and Adams, M. J., "Nonlinear dynamics induced by parallel and orthogonal optical injection in 1550 nm vertical-cavity surface-emitting lasers (vcsels)," *Optics express* **18**(9), 9423–9428 (2010).

[22] Gatare, I., Buesa, J., Thienpont, H., Panajotov, K., and Sciamanna, M., "Polarization switching bistability and dynamics in vertical-cavity surface-emitting laser under orthogonal optical injection," *Optical and Quantum Electronics* **38**(4), 429–443 (2006).

[23] Virte, M., Panajotov, K., Thienpont, H., and Sciamanna, M., "Deterministic polarization chaos from a laser diode," *Nature Photonics* **7**(1), 60–65 (2013).

[24] Gatare, I., Sciamanna, M., Buesa, J., Thienpont, H., and Panajotov, K., "Nonlinear dynamics accompanying polarization switching in vertical-cavity surface-emitting lasers with orthogonal optical injection," *Applied Physics Letters* **88**(10), 101106 (2006).

[25] Valle, A., Gatare, I., Panajotov, K., and Sciamanna, M., "Transverse mode switching and locking in vertical-cavity surface-emitting lasers subject to orthogonal optical injection," *IEEE Journal of Quantum Electronics* **43**(4), 322–333 (2007).

[26] Panajotov, K., Gatare, I., Valle, A., Thienpont, H., and Sciamanna, M., "Polarization-and transverse-mode dynamics in optically injected and gain-switched vertical-cavity surface-emitting lasers," *IEEE journal of quantum electronics* **45**(11), 1473–1481 (2009).

[27] Gatare, I., Panajotov, K., and Sciamanna, M., "Frequency-induced polarization bistability in vertical-cavity surface-emitting lasers with orthogonal optical injection," *Physical Review A* **75**(2), 023804 (2007).

[28] Nizette, M., Sciamanna, M., Gatare, I., Thienpont, H., and Panajotov, K., "Dynamics of vertical-cavity surface-emitting lasers with optical injection: a two-mode model approach," *JOSA B* **26**(8), 1603–1613 (2009).

[29] Sciamanna, M. and Panajotov, K., "Two-mode injection locking in vertical-cavity surface-emitting lasers," *Optics letters* **30**(21), 2903–2905 (2005).

[30] Hong, Y., Spencer, P. S., Rees, P., and Shore, K. A., "Optical injection dynamics of two-mode vertical cavity surface-emitting semiconductor lasers," *IEEE journal of quantum electronics* **38**(3), 274–278 (2002).

[31] Denis-le Coarer, F., Quirce, A., Valle, Á., Pesquera, L., Sciamanna, M., Thienpont, H., and Panajotov, K., "Polarization dynamics induced by parallel optical injection in a single-mode vcsel," *Optics letters* **42**(11), 2130–2133 (2017).

[32] Quirce, A., Pérez, P., Popp, A., Valle, Á., Pesquera, L., Hong, Y., Thienpont, H., and Panajotov, K., "Polarization switching and injection locking in vertical-cavity surface-emitting lasers subject to parallel optical injection," *Optics letters* **41**(11), 2664–2667 (2016).

[33] Quirce, A., Popp, A., Denis-le Coarer, F., Pérez, P., Valle, Á., Pesquera, L., Hong, Y., Thienpont, H., Panajotov, K., and Sciamanna, M., "Analysis of the polarization of single-mode vertical-cavity surface-emitting lasers subject to parallel optical injection," *JOSA B* **34**(2), 447–455 (2017).

[34] San Miguel, M., Feng, Q., and Moloney, J. V., "Light-polarization dynamics in surface-emitting semiconductor lasers," *Physical Review A* **52**(2), 1728 (1995).

[35] Lingnau, B., Shortiss, K., Dubois, F., Peters, F. H., and Kelleher, B., "Universal generation of devil's staircases near hopf bifurcations via modulated forcing of nonlinear systems," *Physical Review E* **102**(3), 030201 (2020).

[36] Lu, Y., Zhang, W., Xu, B., Fan, X., Sun, Y.-T., and He, Z., "Directly modulated vcsels with frequency comb injection for parallel communications," *Journal of Lightwave Technology* **39**(5), 1348–1354 (2021).

[37] Shortiss, K., Lingnau, B., Dubois, F., Kelleher, B., and Peters, F. H., "Harmonic frequency locking and tuning of comb frequency spacing through optical injection," *Optics Express* **27**(25), 36976–36989 (2019).

[38] Doumbia, Y., Malica, T., Wolfersberger, D., Panajotov, K., and Sciamanna, M., "Optical injection dynamics of frequency combs," *Optics Letters* **45**(2), 435–438 (2020).

[39] Doumbia, Y., Malica, T., Wolfersberger, D., Panajotov, K., and Sciamanna, M., "Nonlinear dynamics of a laser diode with an injection of an optical frequency comb," *Optics Express* **28**(21), 30379–30390 (2020).

[40] Doumbia, Y., Wolfersberger, D., Panajotov, K., and Sciamanna, M., "Tailoring frequency combs through vcsel polarization dynamics," *Optics Express* **29**(21), 33976–33991 (2021).

[41] Doumbia, Y., Wolfersberger, D., Panajotov, K., and Sciamanna, M., "Two polarization comb dynamics in vcsels subject to optical injection," in [*Photonics*], **9**(2), 115, Multidisciplinary Digital Publishing Institute (2022).

[42] Doumbia, Y., Wolfersberger, D., Panajotov, K., and Sciamanna, M., "Nonlinear polarization dynamics of vcsel with frequency comb injection," in [*Integrated Photonics Research, Silicon and Nanophotonics*], IF1A–6, Optical Society of America (2021).

[43] Doumbia, Y., Wolfersberger, D., Panajotov, K., and Sciamanna, M., "Optical injection dynamics of vcsel frequency combs," in [*The European Conference on Lasers and Electro-Optics*], cb_p_5, Optical Society of America (2021).